

## A data study of the influence of the equatorial upper stratosphere on northern-hemisphere stratospheric sudden warmings

By L. J. GRAY<sup>1</sup>\*, S. J. PHIPPS<sup>1</sup>, T. J. DUNKERTON<sup>2</sup>, M. P. BALDWIN<sup>2</sup>, E. F. DRYSDALE<sup>1</sup> and M. R. ALLEN<sup>1</sup>

<sup>1</sup>*Rutherford Appleton Laboratory, UK*

<sup>2</sup>*Northwest Research Associates, USA*

(Received 31 May 2000; revised 22 February 2001)

### SUMMARY

Equatorial winds in the stratosphere are known to influence the frequency of stratospheric midwinter sudden warmings. Sudden warmings, in turn, influence the Earth's climate both through their direct influence on polar temperatures and through the temperature dependence of ozone depletion in the lower stratosphere. The conventional (Holton–Tan) explanation for the equatorial influence on sudden warmings is in terms of the equatorial winds in the lower stratosphere (~20–30 km) acting as a waveguide for midlatitude planetary-wave propagation. This study employs stratospheric-temperature analyses and equatorial rocketsonde wind data extending to 58 km to diagnose the relationship between the northern-hemisphere polar temperatures and equatorial zonal winds at all height levels in the stratosphere. In addition to the recognized Holton–Tan relationship linking the polar temperatures to the quasi-biennial oscillation in equatorial winds in the lower stratosphere, a strong correlation of polar temperatures with equatorial winds in the upper stratosphere is found. We suggest that this may be associated with the strength and vertical extent of the westerly phase of the semi-annual oscillation in the upper stratosphere, although the observations alone cannot provide a conclusive, causal relationship. The main diagnostic tools employed are correlation studies and composite analysis. The results underline the need for continued high quality, equatorial wind measurements at all stratospheric levels.

**KEYWORDS:** Interannual variability Northern-hemisphere winter Quasi-biennial oscillation Semi-annual oscillation Stratosphere Stratospheric sudden warming

### 1. INTRODUCTION

The northern hemisphere (NH) stratospheric winter circulation displays substantial interannual variability (Labitzke 1982). Some winters are extremely disturbed and are accompanied by midwinter stratospheric sudden warmings, in which the polar temperature increases by 20 degC or more in just a few days (Andrews *et al.* 1987). In contrast, other winters have fewer warming events and the polar vortex remains cold and undisturbed. Variability associated with stratospheric warmings is the primary source of interannual variability in the NH winter lower stratosphere. The variability of NH winter stratospheric temperatures also appears to be closely coupled to the Arctic oscillation, the leading mode of variability in the troposphere (Thompson and Wallace 1998; Baldwin and Dunkerton 1999).

Global annual-mean temperatures in the lower stratosphere have fallen by ~0.6 degC per decade over recent decades (e.g. WMO 1998). It is important to characterize natural variability if we are to assess how much of the observed temperature trend is directly related to human activity. It is also important because temperature crucially influences the chemical processes that lead to ozone trends in this region. Stratospheric warmings result in a weak, disturbed vortex with warm temperatures and substantial downward transport of ozone-rich air. Conversely, a strong, stable vortex with low temperatures will result in large chemical ozone loss (due to the temperature thresholds for polar stratospheric cloud formation and hence temperature dependence of chlorine activation) and weak transport of ozone (Chipperfield and Jones 1999). A number of

\* Corresponding author: Rutherford Appleton Laboratory, Chilton, Didcot, Oxon. OX11 0QX, UK. e-mail: L.J.Gray@rl.ac.uk

studies have found evidence for long-term changes in the stratospheric circulation, including a strengthening and cooling of the Arctic vortex (Labitzke and van Loon 1995; Zurek *et al.* 1996). Any such changes would, for the reasons just stated, influence the long-term trends in ozone and temperature (Hood *et al.* 1997).

Although stratospheric sudden warmings have been observed and documented for many years, the factors that control their interannual variability are not well understood. An essential requirement for their development is the presence of quasi-stationary planetary-wave disturbances. These waves are generated in the troposphere and propagate upward into the stratosphere, where the wave-one component can be of sufficient amplitude to displace the vortex well away from the pole. Associated with each vortex displacement there is a rapid increase in temperature at the pole (whether or not the vortex is also disrupted).

The correlation between the wintertime average polar temperature and the phase of the quasi-biennial oscillation (QBO) in the lower stratosphere was noted over 20 years ago (Holton and Tan 1980, 1982). The QBO is an oscillation of the equatorial zonal winds in the lower stratosphere between easterlies and westerlies, with an average period of 28 months. The maximum amplitude of the oscillation occurs around 25–30 km. When the equatorial zonal winds at 20–30 km are in an easterly QBO phase, the northern polar vortex is generally warmer and more disturbed by planetary waves, and displacement and/or disruption of the vortex by midwinter warmings is more likely than in the westerly QBO phase (see also Dunkerton and Baldwin 1991; Baldwin and Dunkerton 1998). The conventional explanation for this correlation is that the QBO winds in the lower stratosphere influence the background mean flow, which then affects the propagation of planetary-scale waves (e.g. McIntyre 1982; Holton and Austin 1991; O'Sullivan and Young 1992; O'Sullivan and Dunkerton 1994; Hamilton 1998; Niwano and Takahashi 1998; Baldwin *et al.* 2001). More specifically, the QBO winds in the lower stratosphere determine the position of the zero wind line near the equator, whose associated nonlinear critical layer acts as a wave-guide for the planetary-wave propagation. This results in enhanced poleward heat transfer during an easterly QBO phase and weaker transfer during a westerly phase.

While this mechanism is generally accepted, it has also been recognized that the 'Holton–Tan' two-way distinction between 'warm disturbed easterly phase' and 'cold undisturbed westerly phase' does not always hold up, particularly in late winter (Hamilton 1998; Baldwin *et al.* 2001). Labitzke and van Loon (1988) and Naito and Hirota (1997) have noted that the periods when the Holton–Tan relation holds up well coincide with periods when the 11-year solar cycle is at its minimum phase (defined, for example, by the 10.7 cm solar flux). Conversely, it appears to substantially weaken or reverse during periods of solar maxima. While the solar cycle–QBO and the solar cycle–NH polar temperature links have been studied extensively (e.g. Labitzke and van Loon 1988; Gray and Dunkerton 1990; Teitelbaum and Bauer 1990; Kodera 1991, 1993, 1995; Salby and Shea 1991; Dunkerton and Baldwin 1992; Balachandran and Rind 1995; Rind and Balachandran 1995; Labitzke and van Loon 1996; Naito and Hirota 1997; Haigh 1999; Shindell *et al.* 1999), the precise mechanism that interrelates (1) the QBO, which has its maximum amplitude in the lower-middle equatorial stratosphere (~20–30 km), (2) the observed wintertime lower-stratospheric polar temperatures and (3) the solar cycle, whose primary influence is in the region of the equatorial stratopause (~40–50 km), has yet to be clearly elucidated.

In this paper, we explore the possible links between these three phenomena by examining the relationship between observed polar temperatures and two different equatorial zonal-wind datasets. The first is the long time series of wind observations from

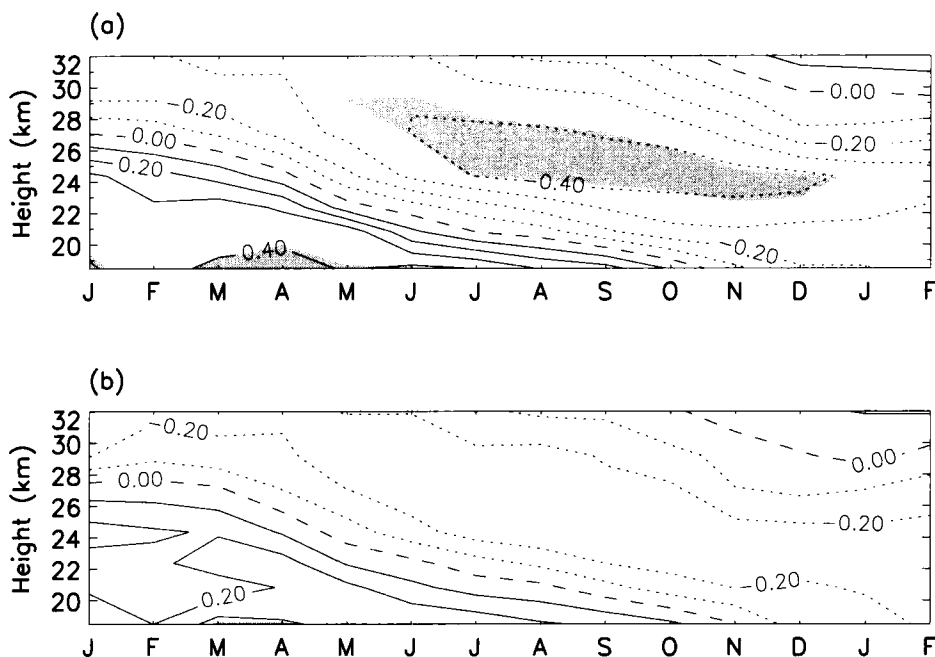


Figure 1. Correlation for the periods (a) 1964–90 and (b) 1955–99 between January–February north-polar temperatures at 24 km and monthly averaged equatorial zonal wind ( $u_{eq}$ ) from radiosonde ascents in each month from January of the previous year to February of the same year. Contour interval is 0.1. Dotted contours denote negative values. The dashed line is the zero contour. Shading indicates values are significant at the 95% confidence level (no values were significant at the 99% confidence level). For details of the significance test applied, see appendix.

radiosonde ascents (Naujokat 1986) for the period 1955–99 that extend to approximately 32 km. The second is a rocketsonde zonal-wind dataset for the period 1964–90 (Dunkerton and Delisi 1997; Dunkerton *et al.* 1998) that extends to 58 km. The rocketsonde dataset, therefore, includes not only the lower-stratospheric winds (20–30 km) usually associated with the observed QBO modulation of the polar temperatures but also the higher altitudes that encompass the stratopause region, where the solar influence is greatest. In section 2 we briefly review the results of correlations between north-polar (NP) temperatures and the lower-stratospheric winds from the radiosonde dataset. In section 3 the rocketsonde dataset is described and a detailed analysis is presented of the relationships between NP temperatures and equatorial winds at all heights to 58 km using the rocketsonde dataset. This analysis includes correlation studies, regression analyses, and composite studies. The main conclusions of the study are presented in section 4.

## 2. RADIOSONDE ANALYSIS

Figure 1(a) shows the correlation over 26 winters 1964–90 between the observed January–February average (JF) NP temperatures at 24 km and the equatorial zonal winds ( $u_{eq}$ ) from radiosonde observations in each month from January of the previous year to February of the same year. The NP temperatures are from the Berlin stratospheric analyses (courtesy K. Labitzke). The time interval 1964–90 is employed here to facilitate comparison with the rocketsonde analysis in the next section. We choose to use JF temperatures since most midwinter warmings occur in these months (and also to maintain consistency with previous studies). The NP temperatures are anti-correlated

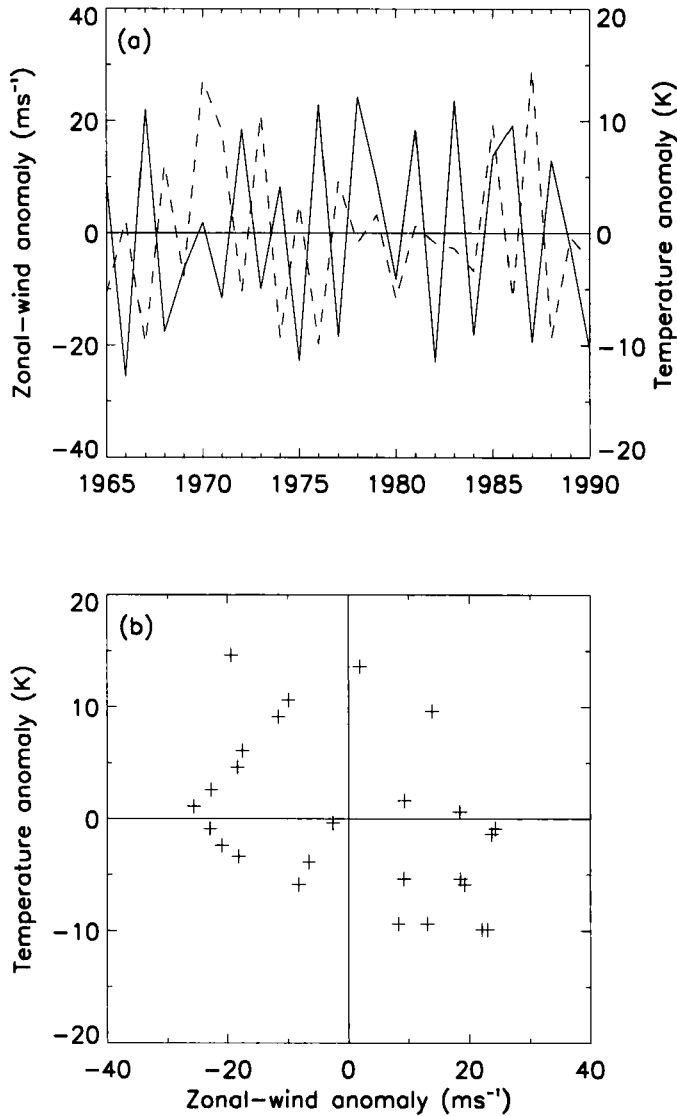


Figure 2. (a) Time series of January–February north-polar temperature anomalies (K) at 24 km ( $\sim 30$  hPa) (dotted line) and equatorial zonal wind ( $u_{eq}$ ) anomalies ( $m s^{-1}$ ) at 24 km in the preceding December (solid line). (b) Scatter plot of the data.

with the lower stratospheric  $u_{eq}$  in the previous months. The region of maximum correlation descends gradually through the atmosphere with time, corresponding to the descent of the QBO wind regimes. The sign of the correlation is consistent with the Holton–Tan mechanism, with easterly (negative)  $u_{eq}$  associated with warm (positive) polar temperatures and vice versa. For the 26-year period 1964–90, the maximum correlation coefficients are of order  $-0.4$ . However, when the correlation is repeated using data from 44 winters (1955–99, see Fig. 1(b)), which is the full extent of the available radiosonde data, the correlation drops in magnitude to only  $\sim -0.25$ .

Figure 2(a) shows the JF NP temperature anomalies at 24 km for the time interval 1964–90 (derived by subtracting the mean value over the period from each data point)

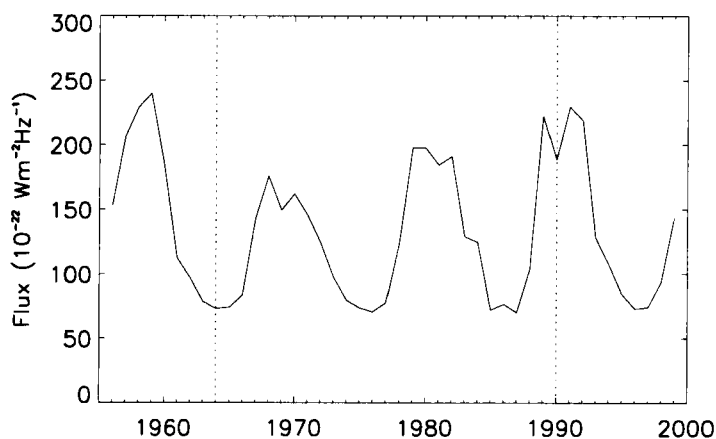


Figure 3. Time series of annual-mean solar 10.7 cm radio flux ( $\times 10^{-22} \text{ W m}^{-2} \text{ Hz}^{-1}$ ). The dotted lines show the start and end of the period for which the rocketsonde data are available.

and the  $u_{\text{eq}}$  anomaly at 24 km over the same time interval. It shows that the Holton–Tan relationship of negative correlation between the two signals holds for certain periods but not others. For example, the two signals are anti-correlated during the periods 1965–68, 1971–78 and 1986–88, but in the intervening years either the opposite is true (e.g. 1969–70, 1980–81 and 1984–85) or there is no apparent relationship (e.g. 1982–83). It is these latter periods that degrade the correlation, resulting in the relatively low correlations seen in Fig. 1. A scatter plot of the data (Fig. 2(b)) further demonstrates the weakness of the resulting correlation.

The difference in correlation displayed by the analysis of the two time intervals in Fig. 1 can be understood in terms of the influence of the solar cycle. Figure 3 shows the time series of 10.7 cm radio flux for 1955–99. Notice that the 1955–99 interval encompasses nearly four complete solar-cycle periods while the 1964–90 interval encompasses only approximately 2.5 cycles with a slight bias towards solar-minimum conditions (the solar maximum around 1968–70 is rather weak). Note also that the time interval 1962–78 originally examined in Holton and Tan’s study was also biased towards solar-minimum conditions (Naito and Hirota 1997). In Fig. 2(a), the periods of Holton–Tan (i.e. negative) correlation tend to coincide with periods under solar-minimum conditions and the periods in which the Holton–Tan relation is reversed (or absent) tend to coincide with periods under solar-maximum conditions. It was Labitzke and van Loon (1988) who first noted this apparent interaction of the 11-year solar cycle with the QBO. In their study of the solar-cycle influence on polar temperatures they separated the observed JF NP temperatures depending on the phase of  $u_{\text{eq}}$  in the lower stratosphere (see also Naito and Hirota 1997). In Fig. 4 we repeat their analysis for the interval 1955–99 to bring it up to date. The winters were classified using  $u_{\text{eq}}$  at 50 hPa (approximately 24 km) in accordance with the criterion used by Labitzke and van Loon. ‘Transition’ years when  $u_{\text{eq}}$  was within the range  $\pm 5 \text{ m s}^{-1}$  were excluded. Note the strong positive correlation ( $r = +0.68$ ) of polar temperatures with the 10.7 cm flux in the west QBO phase and the negative correlation in the east QBO phase. The negative correlation appears to break down in the last few years of Fig. 4(b) and this results in a correlation coefficient of only  $-0.14$  when the whole interval 1955–99 is included in the analysis. However, there was an extremely strong El

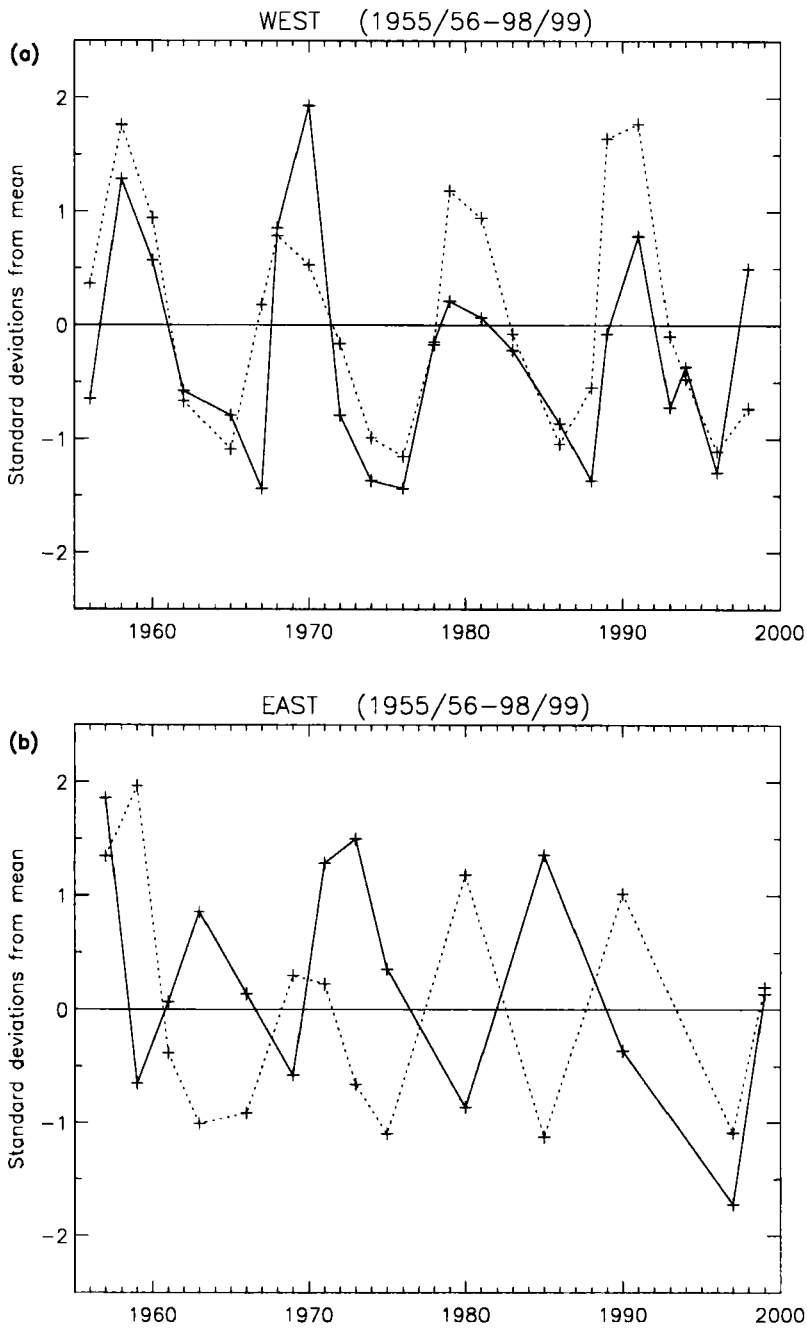


Figure 4. Time series of north-polar temperature anomalies at 24 km ( $\sim 30$  hPa) (solid line) and 10.7 cm radio flux (dotted line). (a) West quasi-biennial oscillation (QBO) phase years, (b) east-phase years. Both signals have been plotted as standard deviations from the mean over the whole time interval to aid comparison.

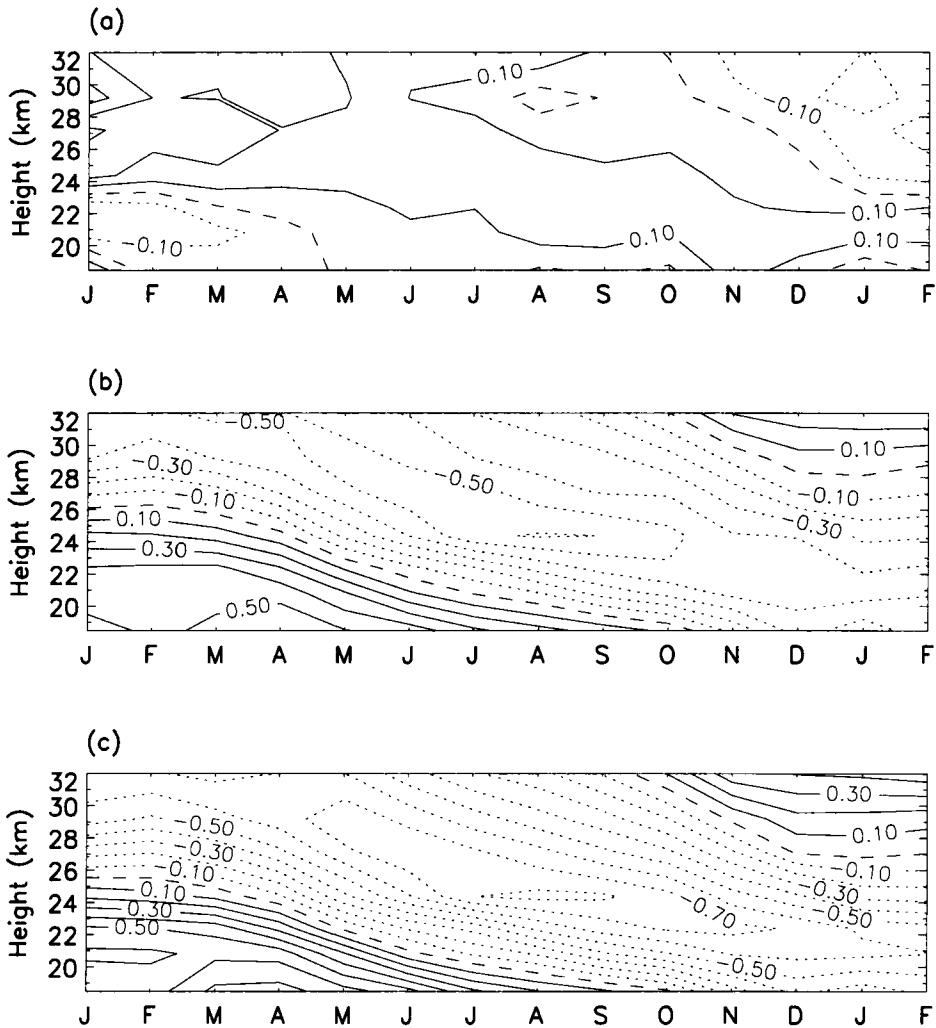


Figure 5. Correlation over the time interval 1955–99 between January–February north-polar temperatures at 24 km and monthly averaged equatorial zonal wind ( $u_{eq}$ ) from radiosonde ascents in each month from January of the previous year to February of the same year. (a) Solar-maximum years, (b) solar-minimum years, (c) solar-minimum years but for time interval 1955–96 only. Contour interval is 0.1. Dotted contours denote negative values. The dashed line is the zero contour. Note that no-confidence levels are estimated as the sampling interval varies in these stratified datasets and hence the autocorrelation of the data cannot be determined (see appendix).

Niño in 1997 (Stockdale *et al.* 1998) which may have influenced the polar temperatures in that year.

In this study we take a slightly different approach to Labitzke and van Loon (1988) since we wish to explore the solar influence on the QBO–polar-temperature relationship rather than the QBO influence on the solar–polar-temperature relationship. We have, therefore, recalculated the QBO–polar-temperature correlations for the time interval 1955–99 shown in Fig. 1(b) after first separating the winters depending on whether the JF 10.7 cm solar flux was less than or greater than the mean for the whole period. Using this criteria we obtain 18 and 25 winters under solar-maximum and solar-minimum conditions, respectively. Under solar-maximum conditions (Fig. 5(a)) there is a small positive correlation in the lower stratosphere suggesting that polar temperatures are

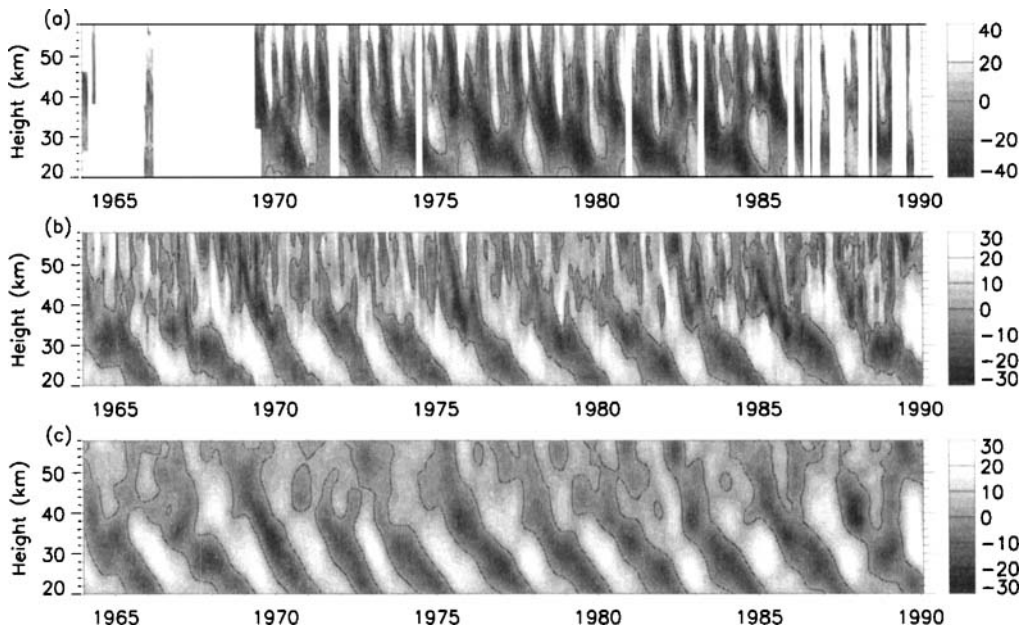


Figure 6. (a) Monthly averaged zonal wind ( $\text{m s}^{-1}$ ) derived from rocketsonde ascents at Kwajalein ( $8^{\circ}\text{N}$ ). (b) Deseasonalized monthly averaged zonal-wind dataset derived by combining data from both Kwajalein and Ascension Island as described in the text. (c) As in panel (b) after passing through a 9–60-month bandpass filter. The zero value is denoted by the contour line.

warmer in the QBO westerly phase than in the QBO easterly phase, i.e. in the opposite sense to the Holton–Tan relation. However, the amplitude of this positive correlation is extremely small. Under solar-minimum conditions (Fig. 5(b)), on the other hand, there is a strong Holton–Tan relationship with a descending region of negative correlation reaching a maximum strength of  $-0.61$  at 24 km in August. If the analysis is repeated for the time interval 1955–96 in order to exclude the strong El Niño event in 1997 this correlation increases in magnitude to  $-0.83$  (Fig. 5(c)).

### 3. ROCKETSONDE ANALYSIS

#### (a) *The data*

Regular rocketsonde ascents were made from Kwajalein ( $8^{\circ}\text{N}$ ) during the period 1969–90 and from Ascension Island ( $8^{\circ}\text{S}$ ) during the periods 1962–77 and 1979–89. Occasional gaps of up to a few months duration are present in both records. In order to obtain a single, unbroken time series of equatorial winds, the monthly averaged data from the two stations were first deseasonalized. This was done by calculating and subtracting the climatological monthly mean at each height and at each station. Gaps of up to three months duration in the records for each station were then filled by linear interpolation. For those heights and months when data were available for both stations, the two datasets were combined by averaging them together. When data were only available from one station, those data were used. In this way, an unbroken time series of deseasonalized ‘proxy equatorial’ ( $8^{\circ}\text{S}$ – $8^{\circ}\text{N}$  averaged) zonal winds was achieved from January 1964 to February 1990 for the height region 20–58 km.

Figure 6(a) shows the time–height cross-section of the raw monthly averaged data from Kwajalein. The QBO is the dominant signal in the lower stratosphere (20–35 km).

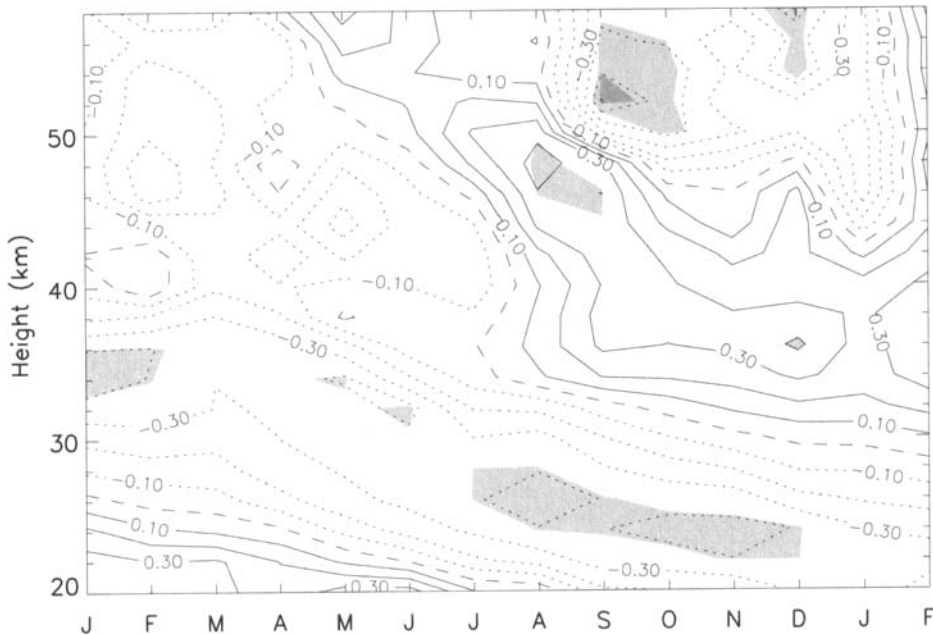


Figure 7. Correlation for the period 1964–90 between January–February north-polar temperatures at 24 km and monthly averaged equatorial zonal wind ( $u_{eq}$ ) from rocketsonde ascents in each month from January of the previous year to February of the same year. Contour interval is 0.1. Dotted contours denote negative values. The dashed line is the zero contour. Light and dark shading indicates values are significant at the 95% and 99% confidence levels, respectively. For details of the significance test applied, see appendix.

The maximum amplitude of the oscillation is at around 25 km, with the wind varying between  $-30 \text{ m s}^{-1}$  and  $+20 \text{ m s}^{-1}$ . Above 35 km the semi-annual oscillation (SAO), with a period of six months, dominates. Figure 6(b) shows the combined Kwajalein and Ascension Island dataset, which was derived as described above. (Note that the SAO has been removed by the deseasonalizing process.) The QBO period is further highlighted in Fig. 6(c) using a 9–60-month bandpass filter.

#### (b) Correlation studies

The correlation study to examine the link between  $u_{eq}$  and JF NP temperatures was repeated using the rocketsonde wind observations to extend the analysis into the upper equatorial stratosphere. Figure 7 shows the correlation at each height and month leading up to January–February (i.e. identical to Fig. 1(a) but using the rocketsonde data). Note first the negative correlation of  $\sim 0.4$  at 20–35 km, which slowly propagates downwards with time. This was the correlation noted by Holton and Tan nearly 20 years ago and below 30 km it is virtually identical to the results of the correlations using radiosonde wind data (Fig. 1(a)).

However, there is also significant correlation at higher levels. In the 30–50 km region there is a positive correlation of  $\sim 0.3$ – $0.4$ , also descending with time. This change in sign of the correlation with height reflects the next incoming phase of the equatorial wind QBO (see Fig. 6). Above 50 km, there is a region of relatively high negative correlation in September/October. At 52 km in September, the correlation reaches  $-0.6$  and is significant at the 99% confidence level. We note here that there can be no suggestion that this high correlation is simply a response of  $u_{eq}$  to the winter polar warming, since the strongest correlation is found between the JF polar temperatures and

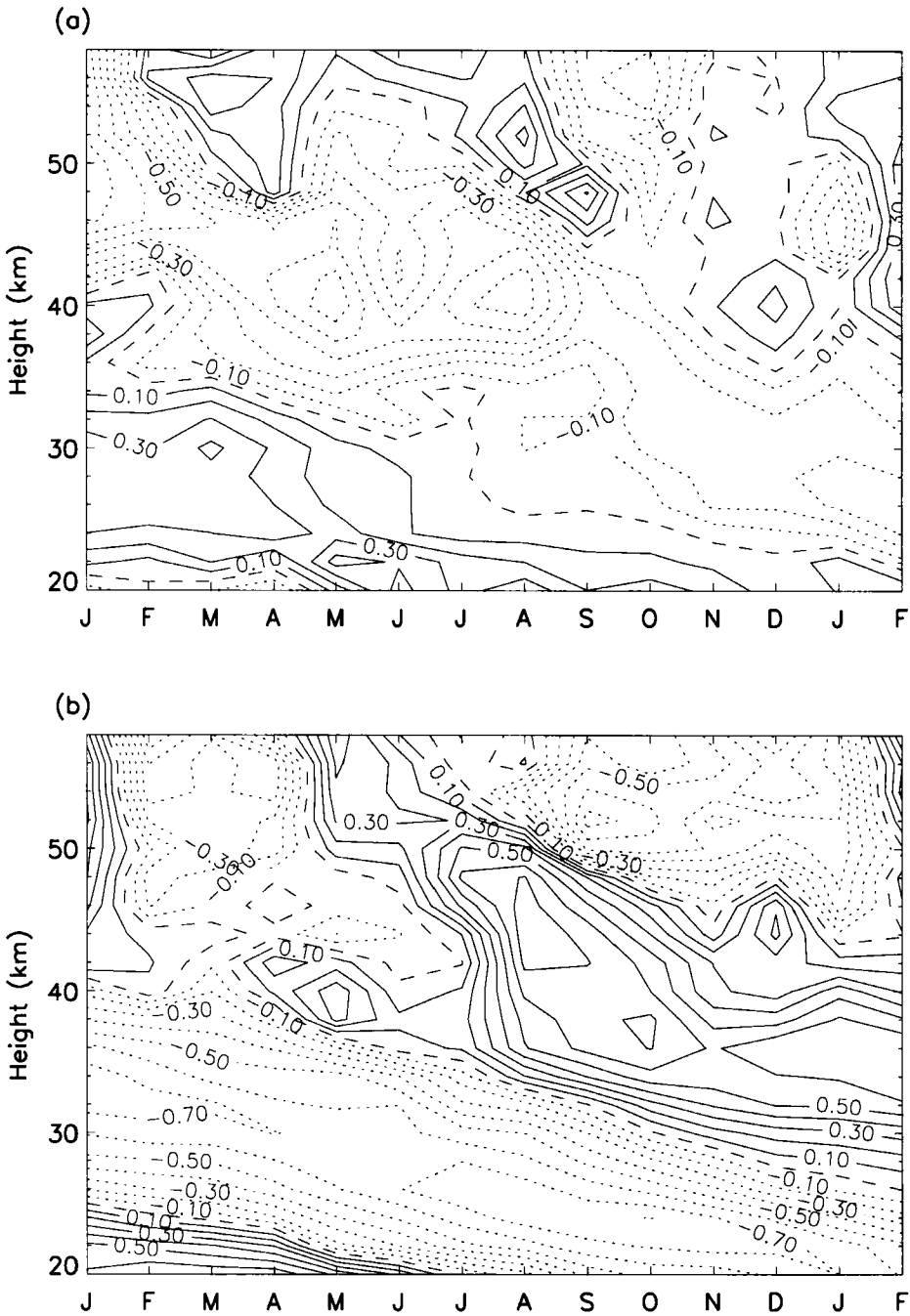


Figure 8. Correlation for the period 1964–90 between January–February north-polar temperatures at 24 km and monthly averaged equatorial zonal wind ( $u_{eq}$ ) from rocketsonde ascents in each month from January of the previous year to February of the same year. (a) Solar-maximum conditions, (b) solar-minimum conditions. Contour interval is 0.1. Dotted contours denote negative values. The dashed line is the zero contour. Note that no-confidence levels are estimated as the sampling interval varies in these stratified datasets and hence the autocorrelation of the data cannot be determined (see appendix).

$u_{eq}$  in the previous September, four to five months before the midwinter warmings take place.

The rocketsonde correlation analysis was also extended to investigate the possible solar-cycle influence, although the limited time span of the rocketsonde data (just over two solar-cycle periods) should be borne in mind in the interpretation of these results. As before, the winters were separated depending on whether the JF 10.7 cm radio flux was less than or greater than the mean for the period, giving 12 and 14 winters in solar-minimum and solar-maximum conditions respectively. The results (Fig. 8) are consistent with the radiosonde analysis (Fig. 5) in showing stronger correlations under solar-minimum conditions than under solar-maximum conditions. The peak correlation amplitudes under solar-minimum conditions are  $-0.80$  at 24 km in October,  $+0.75$  at 44 km in August and  $-0.75$  at 52 km in September.

### (c) Regression analyses

Linear regression analyses were carried out in order to assess the effectiveness of the rocketsonde  $u_{eq}$  at different heights and in different months as a predictor of the wintertime polar temperature. Initially, simple linear regression was used to fit the JF NP temperature to  $u_{eq}$  at (a) 24 km in December (as an indicator of the phase of the QBO in the lower stratosphere), and (b) 52 km in September. The best fit to  $u_{eq}$  at 52 km was found to describe 37% of the variance in the polar temperature. By contrast, the best fit to  $u_{eq}$  at 24 km was found to describe only 16% of the variance.

A series of multiple linear regressions was then carried out in order to find the two parameters that best predict the polar temperatures. In each analysis,  $u_{eq}$  for a given height and month was employed as a fixed parameter, while  $u_{eq}$  for every other available height and month was used in turn as the second parameter. In this way, we sought to maximize the amount of the variance in the polar temperature that could be described. In the first analysis,  $u_{eq}$  at 24 km in December was employed as the fixed parameter. It was found that  $u_{eq}$  at 52 km in September was most effective as the second parameter, with a total of 41% of the variance in the polar temperature being described.

Repeating the analysis with  $u_{eq}$  at 52 km in September as the fixed parameter, it was found that the most effective second parameter was  $u_{eq}$  at 48 km in the same month. A total of 51% of the variance in the polar temperature was described. This is an interesting result on two accounts. Firstly, the greatest additional contribution did not come from the lower stratosphere. Secondly, the two parameters consist of  $u_{eq}$  immediately above and immediately below 50 km in September. In Fig. 7 it can be seen that there is a sharp change in the sign of the correlation at this point. This suggests that the strength of the vertical gradient of  $u_{eq}$  at  $\sim 50$  km in September may be a useful predictor of the NP temperature in the following winter.

In order to investigate this possible link further,  $\partial u_{eq}/\partial z$  was derived from the raw rocketsonde data using centred differences. These values were then deseasonalized and combined in the same manner as that described above for the equatorial winds. The correlation between the JF NP temperature and  $\partial u_{eq}/\partial z$  was found to peak at 50 km in September, with a correlation of  $-0.68$ . Using simple linear regression it was found that  $\partial u_{eq}/\partial z$  at 50 km in September could describe 46% of the variance in the JF NP temperature. The multiple linear regression described above was repeated, using  $\partial u_{eq}/\partial z$  at 50 km in September as the fixed parameter and all possible values of both  $u_{eq}$  and  $\partial u_{eq}/\partial z$  as the second parameter. It was found that  $u_{eq}$  at 44 km in October was most effective as the second parameter, with a total of 62% of the variance in the NP temperatures being described.

These results suggest a link between the JF NP temperatures and  $u_{\text{eq}}$  and its vertical gradient in the upper stratosphere in the preceding September/October. This strong link is evident in Fig. 9(a), which shows the JF NP temperatures for 1965–90 overlaid by  $\partial u_{\text{eq}}/\partial z$  at 50 km in the preceding September. The two signals are reasonably well anti-correlated over most of the period. The years that are less well anti-correlated (e.g. 1971, 1977/78) appear to be randomly distributed and, unlike in Fig. 2(a), do not display a solar-cycle pattern. Unfortunately, the length of the rocketsonde data interval is too short to produce meaningful results if the above analysis is repeated after first separating into solar-minimum and solar-maximum conditions. A comparison of the scatter plot of the data (Fig. 9(b)) with the corresponding plot in Fig. 2(b) for the lower-stratospheric winds ( $u_{\text{eq}}$  at 24 km) clearly demonstrates that the relationship between the JF polar temperature and  $\partial u_{\text{eq}}/\partial z$  at 50 km is stronger than with  $u_{\text{eq}}$  at 24 km.

#### (d) Composites

In Fig. 10 we show a series of latitude–height ‘composite differences’ of JF winds using daily zonally averaged zonal-wind data derived from the National Centers for Environmental Prediction/National Center for Atmospheric Research 1200 UTC heights and temperatures (Kalnay *et al.* 1996). Firstly, composites were derived by averaging together the JF wind distributions from the five warmest and five coldest northern-hemisphere winters between 1964/65 and 1989/90. The appropriate years were selected on the basis of the NP (Berlin) temperatures at 24 km. We do this to highlight the differences in the JF wind distribution between years that exhibit a major warming and those that do not. The ‘cold’ composite minus the ‘warm’ composite is shown in Fig. 10(a). During cold winters the westerly polar vortex is less disturbed by planetary waves and their accompanying warming events and hence there is a strong, high-latitude westerly anomaly, with maximum composite differences of  $35 \text{ m s}^{-1}$  at 32 km ( $\sim 10 \text{ hPa}$ ). There is a small westerly anomaly at the equator, consistent with the Holton–Tan mechanism, peaking at around  $11 \text{ m s}^{-1}$ .

Secondly, the wind distributions were composited on the basis of  $u_{\text{eq}}$  at 24 km in January (using the rocketsonde data, which are virtually identical to the radiosonde data at this level). These composites test the Holton–Tan mechanism whereby the polar temperatures and vortex are influenced by  $u_{\text{eq}}$  in the lower stratosphere. The ‘west QBO’ minus ‘east QBO’ composite differences in Fig. 10(b) show a high-latitude westerly wind anomaly peaking at  $\sim 15 \text{ m s}^{-1}$  at 32 km, consistent with a stronger westerly polar jet during the westerly phase of the QBO at 24 km.

Finally, composites were constructed on the basis of  $\partial u_{\text{eq}}/\partial z$  at 50 km in September (from the rocketsonde data). The difference between the ‘large shear’ and ‘small shear’ years has a maximum amplitude of  $\sim 25 \text{ m s}^{-1}$  at high latitudes (Fig. 10(c)). Hence, years with stronger than average vertical wind shear near the equatorial stratopause in the autumn months tend to be followed by a cold, more stable westerly polar vortex, and vice versa. These composites confirm that, while by no means accounting for the full amplitude of the differences in Fig. 10(a), the composite differences at high latitudes based on  $\partial u_{\text{eq}}/\partial z$  at 50 km in September are substantially larger than those constructed using  $u_{\text{eq}}$  at 24 km.

In Fig. 11 we show the height–time evolution of  $u_{\text{eq}}$  from the rocketsonde data for the ‘warm’ and ‘cold’ composites described above, and the difference between them. The major feature between 40 and 60 km is the SAO, in which  $u_{\text{eq}}$  reverses direction from easterly to westerly and back again on a time-scale of approximately six months. September is the onset of a westerly phase at around 50 km. There is a notable difference

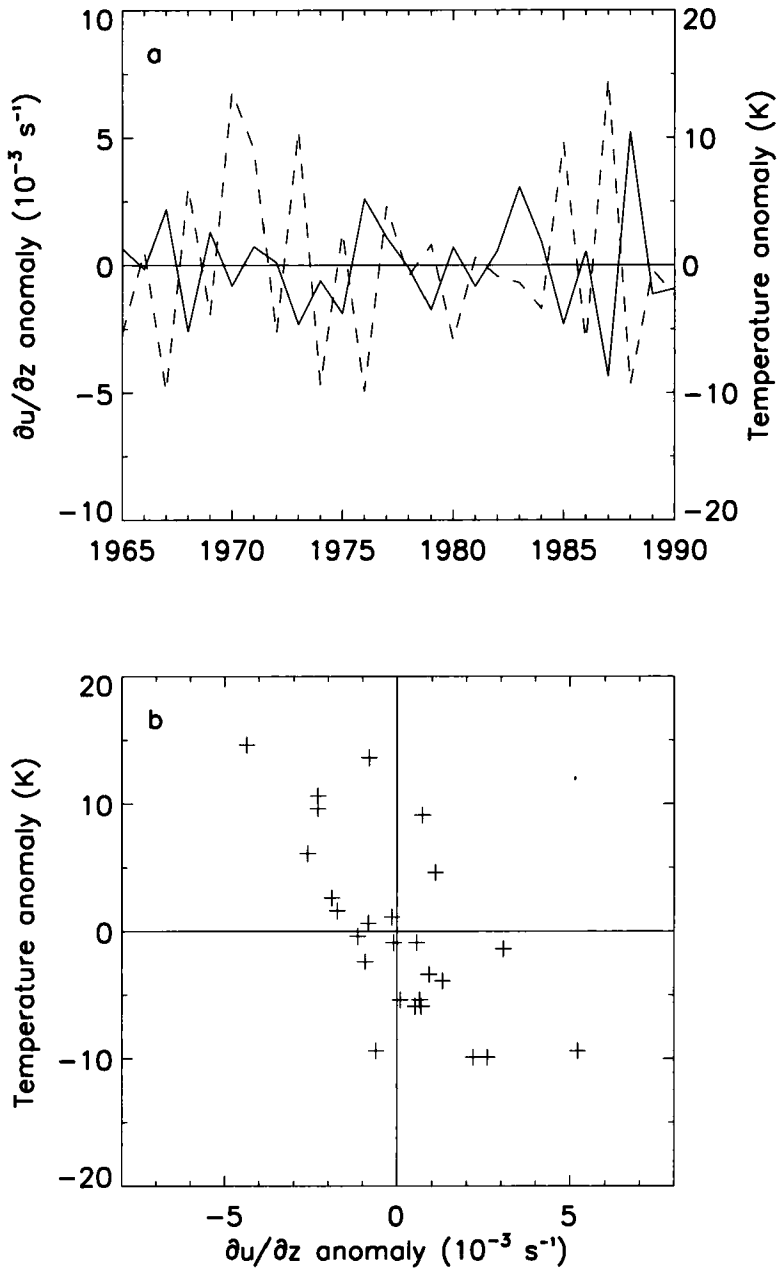


Figure 9. (a) Time series of January–February north-polar temperature anomalies (K) at 24 km ( $\sim 30$  hPa) (dotted line) and anomalies in the vertical gradient of the equatorial zonal wind ( $\partial u_{\text{eq}} / \partial z$ ,  $\times 10^{-3} \text{ s}^{-1}$ ) at 50 km in the preceding September (solid line). (b) Scatter plot of the data.

in the nature of this westerly phase between the ‘warm’ and ‘cold’ composites. In the ‘warm’ composite, the westerly phase extends deeper in the atmosphere, with the zero wind line at its lowest extent in November, reaching  $\sim 30$  km compared with only  $\sim 40$  km in the ‘cold’ composite. This is a result of a more rapid descent of the westerly phase during September and October. The vertical wind shear at  $\sim 50$  km in

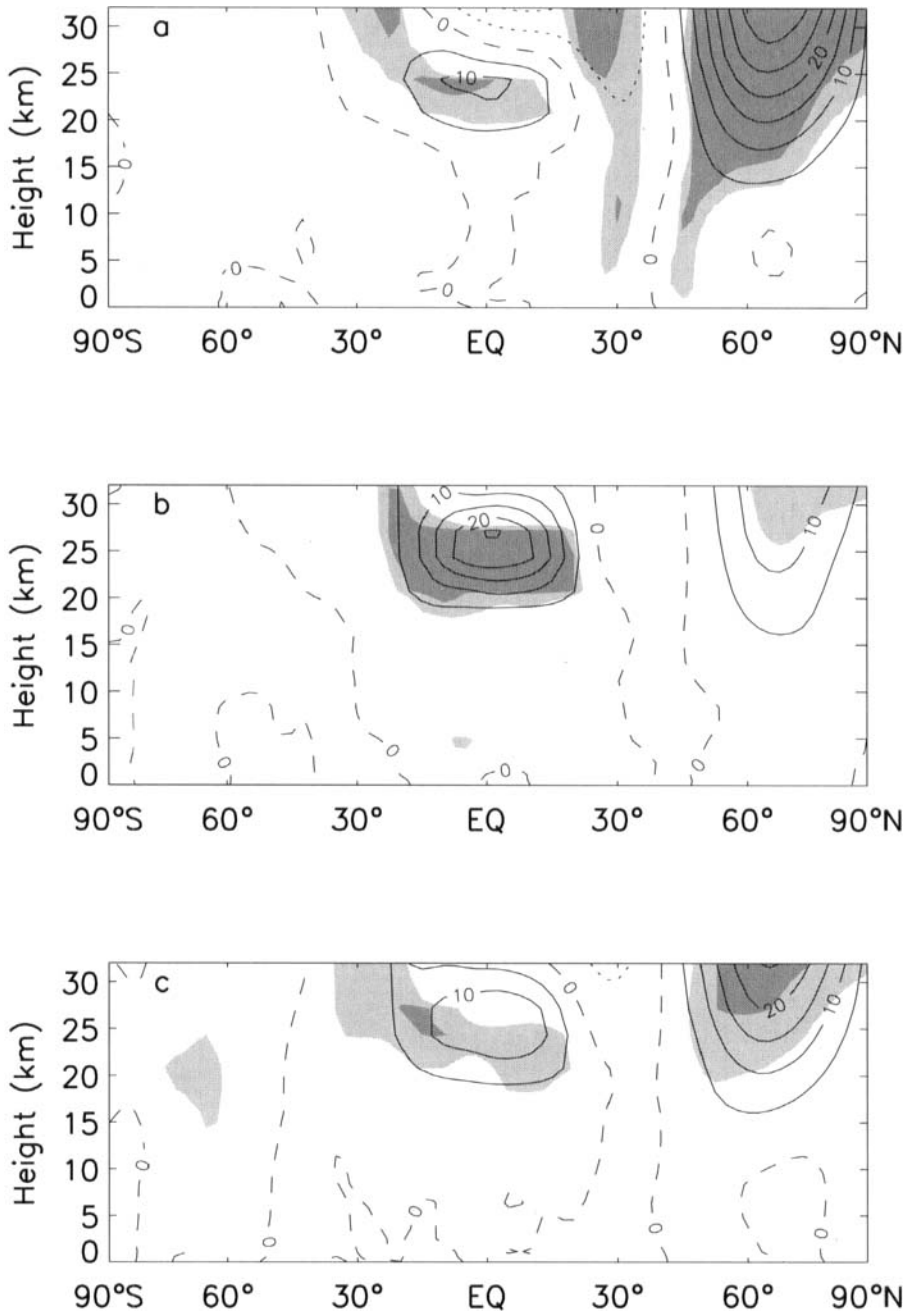


Figure 10. Latitude–height distributions of January–February (JF) zonally averaged zonal wind ( $\text{m s}^{-1}$ ) from the National Centers for Environmental Prediction analyses for the period 1964–90. (a) Composite difference of the five coldest minus five warmest northern-hemisphere winters as determined by the 30 hPa JF north-polar temperatures, (b) composite difference of the five most westerly minus five most easterly quasi-biennial oscillation phase based on the equatorial zonal wind ( $u_{\text{eq}}$ ) at 24 km in the previous December, (c) composite difference of the five strongest minus five weakest  $\partial u_{\text{eq}}/\partial z$  at 50 km in the previous September. Contour interval is  $5 \text{ m s}^{-1}$ . Negative (easterly) values are denoted by dotted contours. Light and dark shading denote regions where values are significant at the 95% and 99% confidence levels respectively. The significances of the values were tested by performing a Student's *t*-test on the difference between the two mean wind distributions.

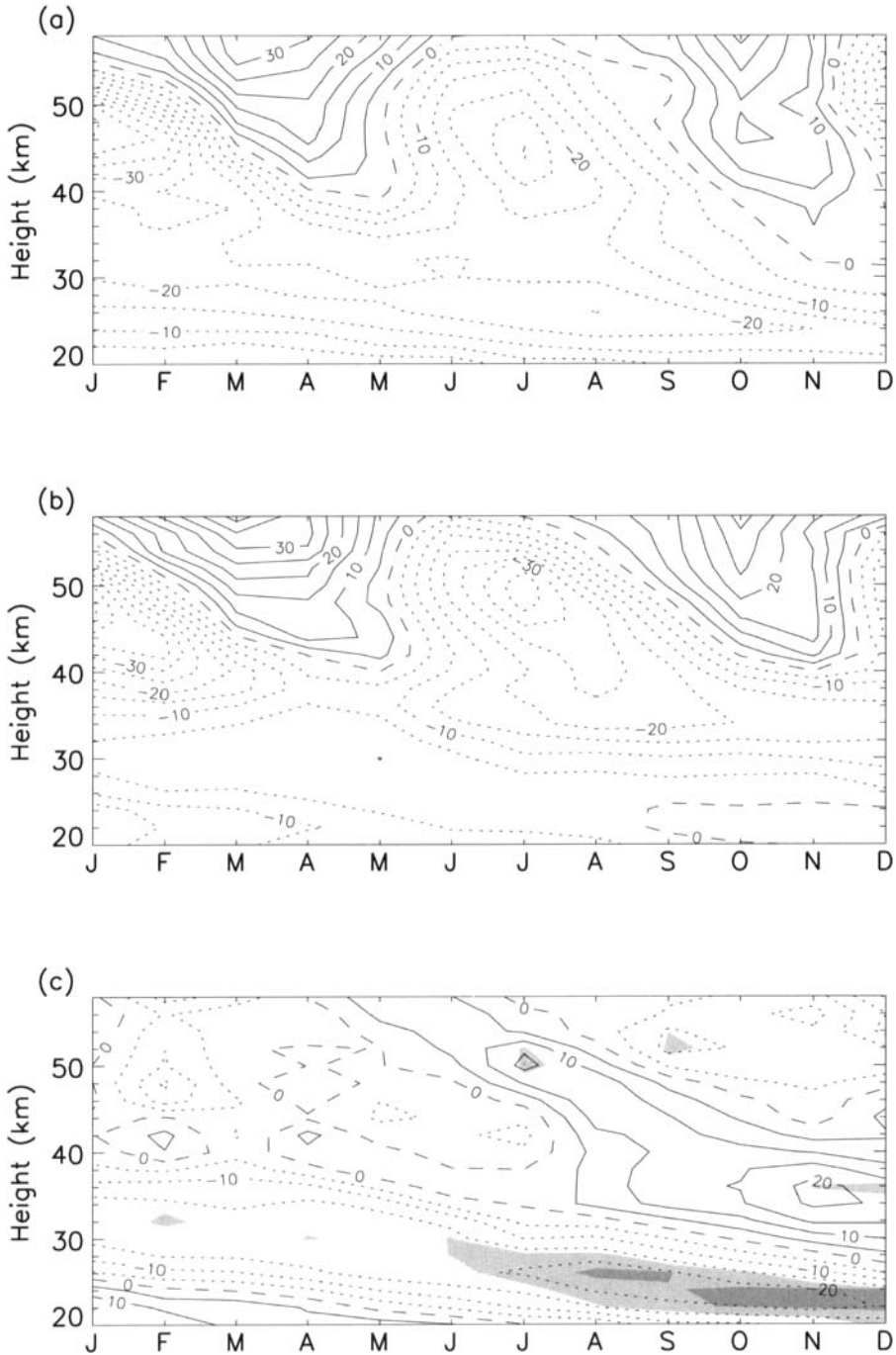


Figure 11. Time series of monthly averaged equatorial zonal wind ( $u_{eq}$ ,  $m s^{-1}$ ) measured by rocketsonde. (a) Composite of five warmest northern-hemisphere winters, as determined using 30 hPa north-polar temperatures, (b) as for panel (a) but for the five coldest winters. (c) The difference between the two composites, i.e. panel (a) minus panel (b). Contour interval is  $5 m s^{-1}$ . Negative (easterly) values are denoted by dotted contours. Light and dark shading denote regions where values are significant at the 95% and 99% confidence levels respectively. The significances of the values were tested by performing a Student's  $t$ -test on the difference between the two mean wind distributions.

September reflects this difference, being weaker in the 'warm' composite than in the 'cold' composite (as we have already noted in the discussion of Fig. 10(c) above).

Figure 11 suggests that the difference between the warm and cold composites may be associated with the relative strength and depth of the SAO westerly phase around September/October. The westerly phase of the SAO arises as a result of vertically propagating westerly phase equatorial waves, e.g. gravity and Kelvin waves (Andrews *et al.* 1987). These waves are able to propagate relatively easily through lower-stratospheric easterlies. However, when the waves reach heights ( $\sim 50$  km) where the background zonal winds are of similar magnitude and direction to their own phase speeds, the waves are unable to propagate further. They are dissipated and their Eliassen–Palm fluxes converge, accelerating the background flow, thus forcing it even more westerly. In this way, the westerly SAO phase gradually descends through the atmosphere with time. The rate of descent of the westerly phase, and hence the vertical wind shear at 50 km is, therefore, dependent on the QBO in the lower stratosphere, since the relative ease of vertical propagation of the waves with a westerly phase speed depends on the wind speed and direction in the lower stratosphere (Lindzen and Holton 1968; Gray and Pyle 1989; Hirota *et al.* 1991; Kennaugh *et al.* 1997). Strong easterlies at 20–30 km allow enhanced penetration of such waves and hence more effective westerly forcing and more rapid descent (and vice versa). The resulting QBO modulation of the zonal wind at these upper levels has been observed in the High Resolution Doppler Imager wind observations (Burrage *et al.* 1996) and is evident in Fig. 6(c) which shows a weak QBO signal extending into the upper stratosphere. It is for this reason, presumably, that we see evidence of a QBO-like variation in  $\partial u_{\text{eq}}/\partial z$  at 50 km in Fig. 9 and a fairly substantial westerly anomaly in the lower equatorial stratosphere in the composite difference of Fig. 10(c), similar to that in Fig. 10(b).

#### 4. CONCLUSIONS

We have presented evidence for a strong correlation between JF NP temperatures and the equatorial wind ( $u_{\text{eq}}$ ) and its vertical shear in the upper stratosphere in the region of the stratopause ( $\sim 50$  km). This suggests an influence on polar winter temperatures from the upper stratosphere, in addition to that from the lower-stratospheric QBO, which is already well documented. This is perhaps not surprising given that the planetary waves believed to be primarily responsible for stratospheric warmings are deep structures that encompass the whole depth of the stratosphere. The equatorial upper stratosphere is also the part of the stratosphere where the solar cycle has a significant influence. Separating the winters into solar-minimum and solar-maximum conditions enhances the derived correlation under solar-minimum conditions but weakens it under solar-maximum conditions (Fig. 5). The maximum correlation between the NP temperatures and  $u_{\text{eq}}$  occurs in the previous September/October (Fig. 7), at the onset of a westerly phase of the SAO. Warm winters appear to be characterized by a westerly SAO phase that is weaker in amplitude and penetrates deeper into the lower stratosphere than in the colder winters (Fig. 11). However, September and October are fairly quiescent months and it may be inappropriate to place undue emphasis on these months. It may be that the mechanism linking the equatorial upper stratosphere and polar temperatures is present throughout the winter months but is less evident later on because of the more disturbed nature of the winter months.

While a data correlation study such as this cannot, on its own, establish a causal relationship nor provide the mechanism for this relationship (if, indeed, one exists) it nevertheless suggests that a better understanding of the equatorial upper stratosphere

and its influence on the polar stratosphere, will be essential if we are to fully understand the interannual variability of NH polar temperatures. The study also highlights the need for continued high-quality wind measurements of the equatorial upper atmosphere. The 1990s has been an unusual decade, with very few midwinter warmings. This may be an indicator of climate change. Unfortunately, our rocketsonde analysis could not be extended into the 1990s because of the lack of data.

## ACKNOWLEDGEMENTS

We thank Professor Michael McIntyre, Professor Keith Shine and an anonymous referee whose interest and comments have greatly improved this paper. We also thank Prof. K. Labitzke for provision of the Berlin Stratospheric temperature analyses and Dr B. Naujokat for the equatorial radiosonde data. The work performed at the Rutherford Appleton Laboratory was supported by the UK Natural Environment Research Council.

## APPENDIX

In Figs. 1 and 7 the significance of each point on the correlation plot was tested by calculating the value of the statistic,  $t = r\sqrt{(N_e - 2)/(1 - r^2)}$ , where  $r$  is the correlation between the two time series and  $N_e$  is the number of independent data points in the time series. In the null case of no correlation, this statistic is distributed like Student's  $t$ -distribution with  $N_e - 2$  degrees of freedom (Press *et al.* 1992). In order to compensate for the autocorrelation of the wind data, the effective sample size  $N_e = N$ , where  $N$  is the actual number of data points in the time series, unless  $\rho_1 > 0$  where  $\rho_1$  is the lag-one autocorrelation coefficient, in which case  $N_e = N\{(1 - \rho_1)/(1 + \rho_1)\}$  (Wilks 1995).

## REFERENCES

- |   |      |  |
|---|------|--|
| Andrews, D. G., Holton, J. R. and Leovy, C. B.  | 1987 | <i>Middle atmosphere dynamics</i> . Academic Press, London, UK   |
| Balachandran, N. K. and Rind, D.  | 1995 | Modeling the effects of UV variability and the QBO on the troposphere stratosphere system. Part I: The middle atmosphere. <i>J. Climate</i> , <b>8</b> , 2058–2079 |
| Baldwin, M. P. and Dunkerton, T. J.   | 1998 | Quasi biennial modulations of the southern hemisphere stratospheric polar vortex. <i>Geophys. Res. Lett.</i> , <b>25</b> , 3343–3346                               |
|   | 1999 | Propagation of the Arctic Oscillation from the stratosphere to the troposphere. <i>J. Geophys. Res.</i> , <b>104</b> , 30937–30946                                 |
| Baldwin, M. P., Gray, L. J., Dunkerton, T. J., Hamilton, K., Haynes, P. H., Randel, W. J., Holton, J. R., Alexander, M. J., Hirota, I., Horinouchi, T., Jones, D. B. A., Kinnersley, J. S., Marquardt, C., Sato, K. and Takahashi, M. | 2001 | The quasi biennial oscillation. <i>Rev. Geophys.</i> , <b>39</b> , 179–229   |
| Burrage, M. D., Vincent, R. A., Mayr, H. G., Skinner, W. R., Arnold, N. F. and Hays, P. B.  | 1996 | Long-term variability in the equatorial middle atmosphere zonal wind. <i>J. Geophys. Res.</i> , <b>101</b> , 12847–12854   |
| Chipperfield, M. P. and Jones, R. L.  | 1999 | Relative influence of atmospheric chemistry and transport on Arctic ozone trends. <i>Nature</i> , <b>400</b> , 551–554   |
| Dunkerton, T. J. and Baldwin, M. P.   | 1991 | Quasi biennial modulation of planetary scale fluxes in the northern hemisphere winter. <i>J. Atmos. Sci.</i> , <b>48</b> , 1043–1061                               |
|   | 1992 | Modes of interannual variability in the stratosphere. <i>Geophys. Res. Lett.</i> , <b>19</b> , 49–52   |
| Dunkerton, T. J. and Delisi, D. P.  | 1997 | Interaction of the quasi biennial oscillation and the stratopause semiannual oscillation. <i>J. Geophys. Res.</i> , <b>102</b> , 26107–26116                       |

- Dunkerton, T. J., Delisi, D. P. and Baldwin, M. P. 1998 Middle atmosphere cooling trend in historical rocketsonde data. *Geophys. Res. Lett.*, **25**, 3371–3374
- Gray, L. J. and Dunkerton, T. J. 1990 Seasonal cycle modulations of the equatorial QBO. *J. Atmos. Sci.*, **47**, 2431–2451
- Gray, L. J. and Pyle, J. A. 1989 A two dimensional model of the quasi-biennial oscillation of ozone. *J. Atmos. Sci.*, **46**, 203–220
- Haigh, J. D. 1999 A GCM study of climate change in response to the 11-year solar cycle. *Q. J. R. Meteorol. Soc.*, **125**, 871–892
- Hamilton, K. 1998 Effects of an imposed quasi biennial oscillation in a comprehensive troposphere stratosphere mesosphere general circulation model. *J. Atmos. Sci.*, **55**, 2393–2418
- Hirota, I., Sakurai, T. and Gille, J. C. 1991 Kelvin waves near the equatorial stratopause as seen in SBUV ozone data. *J. Meteorol. Soc. Jpn.*, **69**, 179–186
- Holton, H. and Austin, J. 1991 The influence of the equatorial quasi-biennial oscillation on sudden stratospheric warmings. *J. Atmos. Sci.*, **48**, 607–618
- Holton, H. and Tan, H.-C. 1980 The influence of the equatorial quasi-biennial oscillation on the global circulation at 50 mb. *J. Atmos. Sci.*, **37**, 2200–2208
- 1982 The quasi-biennial oscillation in the northern hemisphere lower stratosphere. *J. Meteorol. Soc. Jpn.*, **60**, 140–148
- Hood, L. L., McCormack, J. P. and Labitzke, K. 1997 An investigation of dynamical contributions to midlatitude ozone trends in winter. *J. Geophys. Res.*, **102**, 13079–13093
- Kalnay, M. E., Kanamitsu, M., Kistler, R., Collins, W., Deaven, D., Gandin, L., Iredell, M., Saha, S., White, G., Woollen, J., Zhu, Y., Leetmaa, A., Reynolds, R., Chelliah, M., Ebisuzaki, W., Higgins, W., Janowiak, J., Mo, K.C., Ropelewski, W., Wang, J., Jenne, R. and Joseph, D. 1996 The NCEP/NCAR Reanalysis Project. *Bull. Am. Meteorol. Soc.*, **77**, 437–471
- Kennaugh, R., Ruth, S. L. and Gray, L. J. 1997 Modeling quasi-biennial variability in the semi-annual double peak. *J. Geophys. Res.*, **102**, 16169–16187
- Kodera, K. 1991 The solar and equatorial QBO influences on the stratospheric circulation during the early northern hemisphere winter. *Geophys. Res. Lett.*, **18**, 1023–1026
- 1993 Quasi decadal modulation of the influence of the equatorial quasi biennial oscillation on the north polar stratospheric temperatures. *J. Geophys. Res.*, **98**, 7245–7250
- 1995 On the origin and nature of the interannual variability of the winter stratospheric circulation in the northern hemisphere. *J. Geophys. Res.*, **100**, 14077–14087
- Labitzke, K. 1982 On the interannual variability of the middle stratosphere during the northern winters. *J. Meteorol. Soc. Jpn.*, **60**, 124–139
- Labitzke, K. and van Loon, H. 1988 Association between the 11-year solar cycle, the QBO and the atmosphere. Part I: The troposphere and stratosphere in northern hemisphere in winter. *J. Atmos. Terr. Phys.*, **50**, 197–206
- 1995 A note on the distribution of trends below 10 hPa: The extratropical northern hemisphere. *J. Meteorol. Soc. Jpn.*, **73**, 883–889
- 1996 The signal of the 11-year sunspot cycle in the upper troposphere lower stratosphere. *Space Sci. Revs.*, **80**, 393–410
- Lindzen, R. S. and Holton, J. R. 1968 A theory of the quasi biennial oscillation. *J. Atmos. Sci.*, **25**, 1095–1107
- McIntyre, M. E. 1982 How well do we understand the dynamics of stratospheric warmings? *J. Meteorol. Soc. Jpn.*, **60**, 37–65
- Naito, Y. and Hirota, I. 1997 Interannual variability of the northern winter stratospheric circulation related to the QBO and the solar cycle. *J. Meteorol. Soc. Jpn.*, **75**, 925–937
- Naujokat, B. 1986 An update of the observed quasi biennial oscillation of the stratospheric winds over the tropics. *J. Atmos. Sci.*, **43**, 1873–1877
- Niwano, M. and Takahashi, M. 1998 The influence of the equatorial QBO on the northern hemisphere winter circulation of a GCM. *J. Meteorol. Soc. Jpn.*, **76**, 453–461

- O'Sullivan, D. and Dunkerton, T. J. 1994 Seasonal development of the extratropical QBO in a numerical model of the middle atmosphere. *J. Atmos. Sci.*, **51**, 3706–3721
- O'Sullivan, D. and Young, R. E. 1992 Modeling the quasi biennial oscillation's effect on the winter stratospheric circulation. *J. Atmos. Sci.*, **49**, 2437–2448
- Press, W. H., Teukolsky, S. A., Vetterling, W. T. and Flannery, B. P. 1992 *Numerical recipes in FORTRAN: The art of scientific computing*. Cambridge University Press
- Rind, D. and Balachandran, N. K. 1995 Modeling the effects of UV variability and the QBO on the troposphere stratosphere system. Part II: The troposphere. *J. Climate*, **8**, 2080–2095
- Salby, M. and Shea, D. 1991 Correlations between solar activity and the atmosphere: An unphysical explanation. *J. Geophys. Res.*, **96**, 22579–22595
- Shindell, D. T., Rind, D., Balachandran, N. K., Lean, J. and Lonergan, P. 1999 Solar cycle variability, ozone and climate. *Science*, **284**, 305–308
- Stockdale, T. N., Anderson, D. L. T., Alves, J. O. S. and Balmaseda, M. A. 1998 Global seasonal rainfall forecasts using a coupled ocean-atmosphere model. *Nature*, **392**, 370–373
- Teitelbaum, H. and Bauer, P. 1990 Stratospheric temperature eleven year variation: Solar cycle effect or stroboscopic effect? *Ann. Geophys.*, **8**, 239–242
- Thompson, D. W. J. and Wallace, J. M. 1998 The Arctic oscillation in the wintertime geopotential height and temperature fields. *Geophys. Res. Lett.*, **25**, 1297–1300
- Wilks, D. S. 1995 *Statistical methods in the atmospheric sciences*. Academic Press, San Diego, California, USA
- WMO 1998 'Scientific Assessment of Ozone Depletion; 1998'. World Meteorological Organization, Geneva, Switzerland
- Zurek, R. W., Manney, G. L., Miller, A. J., Gelman, M. E. and Nagatani, R. M. 1996 Interannual variability of the north polar vortex in the lower stratosphere during the UARS mission. *Geophys. Res. Lett.*, **23**, 289–292